Terr. Atmos. Ocean. Sci., Vol. 19, No. 3, 241-255, June 2008 doi: 10.3319/TAO.2008.19.3.241(T)

An Electric Resistivity Study of the Chelungpu Fault in the Taichung Area, Taiwan

Ping-Hu Cheng[1, *], Yueh-Iuan Ger[1], and Szu-Lin Lee[1]

[1] *Institute of Geophysics, National Central University, Chung-Li, Taiwan, ROC*

Received 28 December 2006, accepted 6 August 2007

ABSTRACT

We conducted an electric resistivity survey consisting of six resistivity image profilings and several resistivity measurements on outcrops of strata in the Taichung area to investigate the subsurface structures of the Chelungpu fault. Three magnetotelluric sounding results are added to infer rock formations at depth. Based on the resistivity measurements on outcrops of the strata and the correlations between the interpretative resistivity structures and the rock formations recognized from drilling cores and the outcrops of the strata, the resistivity spectra of rock formations are obtained, and the geological structures are deduced.

The results indicate that the Chelungpu fault is a complex fault system consisting of two major thrusts and several minor faults in the Taichung area. The two major thrusts are the main shear zone in the west and the Chi-Chi earthquake rupture in the east of the fault system. They are 300 - 800 m apart on the ground surface. The main shear zone dips eastwardly at an angle of 20° ~ 60° and has a cumulate throw of several thousands meters. The Chi-Chi earthquake rupture was developed in the Cholan Formation in shallow depth. It dips 40° ~ 60° eastwardly and has a cumulate throw of several tens of meters indicating faulting movements had occurred many times prior to the Chi-Chi earthquake. The Chi-Chi earthquake rupture may become the dominant active fault zone in the northern segment of the Chelungpu fault system.

Key words: Electric resistivity method, Resistivity image profiling, Chelungpu fault, Active fault in Taichung

Citation: Cheng, P. H., Y. I. Ger, and S. L. Lee, 2008: An electric resistivity study of the Chelungpu fault in the Taichung area, Taiwan. Terr. Atmos. Ocean. Sci., 19, 241-255, doi: 10.3319/TAO.2008.19.3.241(T)

1. INTRODUCTION

The Taichung area is located in west-central Taiwan where buildings were seriously destroyed and the ground was greatly disturbed by the 1999 Chi-Chi earthquake. This earthquake was generated by the reactivation of the Chelungpu fault. This fault was suggested to be a thrust fault with easterly Neogene formations riding on westerly Quaternary formations along the base of the hills in west-central Taiwan and to be the southern extension of the Sanyi fault (Meng 1963; Chang 1971; Ho and Chen 2000; Chen et al. 2001; Chen et al. 2003). Before the Chi-Chi earthquake, only a few outcrops of the fault had been found and most of the fault line could not be traced due to weathering, collapse and coverage by debries. During the Chi-Chi earthquake, this fault was reactivated with the hanging wall lifted about 1 - 4 meters above the footwall generally (Lee et al. 1999; Huang et al. 2000; Lin et al. 2000). The surface ruptures showed that the fault is more complex than the previously suggested. It has a wide fault zone consisting of several ruptures and fractures. In some places, it is accompanied by folds and a back thrust. A large portion of the major surface ruptures appears along the base of the Western Foothills where the Pliocene Chinshui Shale westwardly thrusted onto the Quaternary formations, as the previous model had suggested. It is said that the boundary between the Chinshui Shale and the Quaternary formations is a typical contact along the Chelungpu fault. But in the Taichung area, the surface ruptures induced by the 1999 Chi-Chi earthquake (SRICCE) appeared in the late Pliocene Cholan Formation on the slope of the hills located to the east of the base of the Western Foothills. No visible displacement was found along the base of the hills, or along the terrace scarp, except in the southern part of the study area where the Chinshui

* *Corresponding author*
E-mail: Pynhu@ncu.edu.tw

Shale thrusts westwards on the alluvium. Two cores were taken from the Fengyuan well located 4 km to the north of the study area to study the Chelungpu fault. The Fengyuan well is an inclined borehole dipping 50° westward. The cores indicated that the rock formations are Quaternary terrace deposits, Pliocene Chinshui Shale and Mio-Pliocene Kueichulin Formation from top to bottom. Several fracture zones existed in the latter two formations. The major Chelungpu fault zone was recognized as being located at the bottom of the Chinshui Shale, which was underlain by the older Kueichulin Formation at a drilling depth of 225 m (172 m in vertical depth) (Huang et al. 2002; Tanaka et al. 2002). This fault contact is different from the typical model of the Chelungpu fault. A core drilled at the site of TCDP (Fig. 1) showed that the fault zone associated with the 1999 Chi-Chi earthquake is located at the bottom of the Chinshui Shale, which is also underlain by the Kueichulin Formation. At the TCDP site, the Kueichulin Formation is underlain by the Cholan Formation; such an outcome is indicative of a thrust fault. The depth of which was 1707 m. Two questions are then raised: (1) Where is the outcrop of this fault found at 1707 m beneath the TCDP site? (2) Is there any geological structure beneath the foot of the terrace and hills? The intention of this study is to find the answers to these questions using geoelectric resistivity structures.

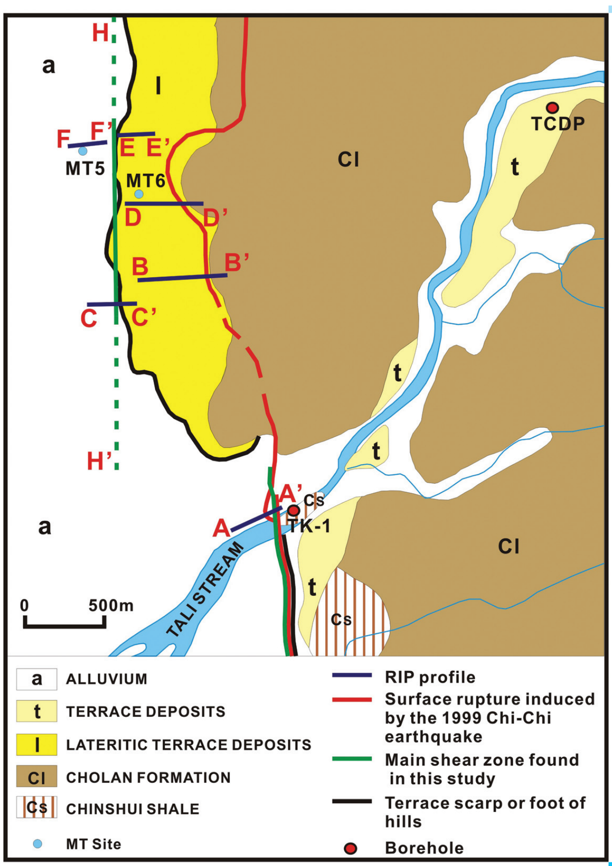

Fig. 1. Geological map of the study area (modified from Ho and Chen 2000) and the locations of the RIP profiles and the MT sites. H-H' is the main shear zone of the Chelungpu fault system found in this study.

2. GEOLOGICAL SETTING

The study area is covered with the Quaternary and the Neogene formations with boundaries generally trending N-S (Fig. 1). From west to east, they are the alluvium, the lateritic terrace deposits, and the Cholan Formation. A small portion of the Chinshui Shale outcrops in the south of the study area. The alluvium is composed of clay, silt, sand, and gravel. The late Pleistocene lateritic terrace deposits are composed largely of unconsolidated gravel with flat-lying sandy or silty lenses. The late Pliocene Cholan Formation is composed of sandstone, shale, and mudstone dominantly. The Pliocene Chinshui Shale is composed largely of shale and a few siltstone and mudstone layers (Ho 1975).

The boundary between the alluvium and the lateritic terrace deposits is also a topographic boundary, the eastern side being an area of terrace and hills while the western side is a plains area. The outcrops of the strata show that the alluvium is undisturbed or little disturbed in the plains area. The lateritic terrace deposits have been tilted, folded and dragged near the terrace scarp. The Cholan Formation dips eastwardly at an angle of 20° - 40° in the hills area. To the east of the study area, the Cholan Formation is overlain by the Toukoshan Formation which is a Pleistocene formation of massive conglomerate containing a few thin sandy beds.

3. METHOD

The technique of electric resistivity image profiling (RIP) with a pole-pole electrode configuration was used in this study as it has a high data density suitable for high resolution interpretation. Basically, it is a four-electrode configuration. A current electrode and a potential electrode, called the sounding electrodes, are set on the surface of the profile to be investigated, while the other two electrodes, also current and potential electrodes, called the remote electrodes, are fixed at distance both from the profile and one another (Fig. 2a).

In practice, many electrodes were arranged on the surface of the profile at equal intervals to enable automatic changing of the sounding electrodes (Fig. 2b). To start, the first electrode was used as the sounding current electrode, and then the second electrode, the third electrode and so on until eventually the (N + 1)th electrode was used in turn as the sounding potential electrode. In this way the first sequence of N data was obtained, where N was the number of measured layers. The largest sounding electrode-spacing was Nl for an electrode interval l. Afterwards, the second electrode was used as the sounding current electrode, and the third electrode, then the fourth electrode and so on until

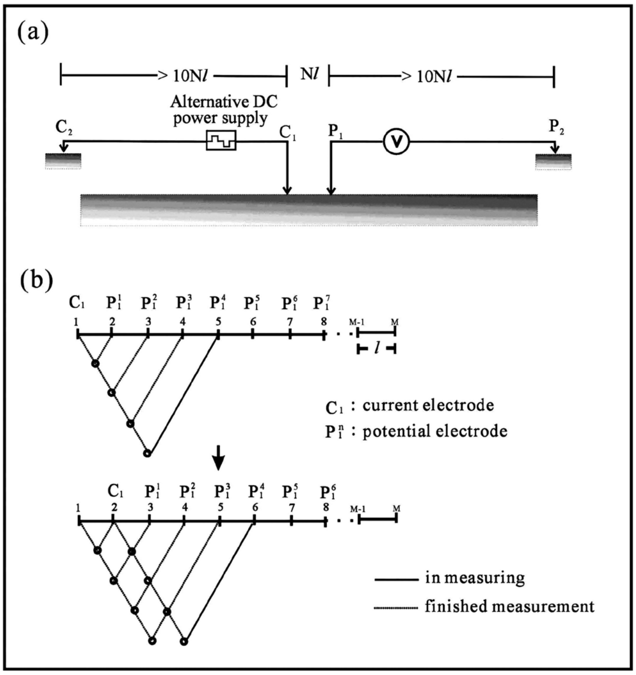

Fig. 2. Electrode configuration of the pole-pole array used in RIP. (a) The sounding electrodes C_1 and P_1 are arranged on the surface of the profile to be investigated. They have a electrode-spacing varying from *l* to N*l*. The remote electrodes C_2 and P_2 are fixed at distance from the profile. (b) A number of electrodes are arranged on the surface of the profile to enable the automatic changing of the sounding electrodes.

eventually the (N + 2)th electrode was used in turn as the sounding potential electrode for N measured layers. In this way, the second sequence of N data was obtained. Similarly, the data gathering continued with the third then the fourth electrodes etc., being used as the initial sounding current electrodes for their respective sequences of N successive sounding potential electrodes (if applicable) until the (M - 1)th electrode was used in turn as the sounding current electrode. Accordingly, a set of RIP data with N measured layers and M sounding electrodes was obtained.

A set of RIP data is usually displayed in the form of apparent resistivity pseudosection. The psudosection is arrived at by plotting each apparent resistivity at a point that corresponds to the mid-point of the sounding electrodes, which serves as the abscissa, and the sounding electrode-spacing, which serves as the ordinate (pseudodepth). Theoretically, the depth of an investigation is proportional to electrode-spacing. Hence, apparent resistivity for the shorter electrode-spacings is the response of shallow strata, while apparent resistivity for larger electrode-spacings is the response from deeper strata. An apparent resistivity pseudosection looks like an image of the bulk resistivity distribution of the formations. Apparent resistivity is not the true resistivity of a place, but rather an equivalent resistivity of the formations in the electrode geometry. The true resistivity of the strata, however, can be obtained with the proper interpretation.

The RIP data were interpreted using the 2-D inversion method as faults can be regarded as 2-D structures. The forward part of the 2-D inversion program used in this study is based on the finite element method and the inverse part is based on the least-squares optimization technique (deGroot-Hedlin and Constable 1990; Tong and Yang 1990; Loke and Barker 1996)

4. RESULTS

Six RIP data sets of A-A', B-B', C-C', D-D', E-E', and F-F' profiles were obtained in the Taichung area. The locations of these profiles are shown in Fig. 1. The measured data and the interpretative results of these profiles are described in the following subsections.

4.1 Profile A-A'

The N70°E trending Profile A-A' is situated on the northern side of the Tali Stream in the south of the study area (Fig. 1). It has a length of 410 m and crosses the surface rupture induced by the 1999 Chi-Chi earthquake (SRICCE) (denoted by F_{cc} in Fig. 3c), a scarp of about one meter high, 260 m from the western end of the profile. Forty-two sounding electrodes placed at 10-m equi-intervals were used in the measuring. The measured data and the interpretative results of this profile are shown in Fig. 3. The interpretative model (Fig. 3c) has a RMS relative error of 7.4% indicating medium fit between the measured and the calculated apparent resistivities, and implying that the results are acceptable. Figure 3c shows that the strata can be divided into two parts reflecting different resistivity structures. The dividing boundary F is an east dipping zone beneath the SRICCE as shown in Fig. 3. The ground in the western part is composed of three layers giving a high-medium-high resistivity pattern from top to bottom. In contrast, the ground in the eastern part is composed mainly of a thick low resistivity layer with a thin high resistivity layer at the top. The dividing boundary appears to be the subsurface rupture associated with the Chi-Chi earthquake.

The top layer of the western part has a resistivity of 150 - 600 Ω-m. It can be correlated to the gravel layer of the alluvium that appears on the banks of the Tali Stream. Based on the geological setting and the resistivity spectra of rocks including the resistivity measured on the outcrops of the formations around the study area (Keller and Frischknecht 1966; Nabighian 1988; Cheng 1990; Ho and Chen 2000; Cheng et al. 2002), the middle layer is interpreted to be a layer of sandy alluvium as it has a resistivity of 30 - 150 Ω-m, and the bottom layer is interpreted to be the late Pleistocene gravel beds because of its high resistivity at 300 - 2000 Ω-m.

The top layer of the eastern part has a resistivity of 150 - 600 Ω-m. It can also be correlated to the gravel layer of the alluvium as it is in the western part. The bottom layer has a very-low resistivity of 5 - 40 Ω-m and is interpreted to be the Chinshui Shale for its very low resistivity characteristics that match those measured on outcrops of the Chinshui Shale exposed on the stream bed. This interpretation is consistent with the drilling results from TK-1 which is located at the eastern end of the profile (Fig. 1). The core of TK-1 taken from the ground surface to a depth of 300 m shows that the rock is shale in the upper part which is underlain by gravel beds at a depth of 130 m. The shale was confirmed to be the Chinshui Shale. The gravel beds are suggested to be late Pleistocene.

The geological section deduced from the resistivity structures is shown in Fig. 3d. It shows that the Chinshui Shale thrusted onto the alluvium and the late Pleistocene gravel beds beneath the fault scarp presenting typical contact for the Chelungpu fault. Therefore, we call this fault as being the main fault zone for the Chelungpu fault system. To the west of the fault, the strata seem to be undisturbed.

4.2 Profile B-B'

Profile B-B' has a length of 630 m trending in N85°E direction in the central part of the study area (Fig. 1). It consists of 64 sounding electrodes at equi-intervals of 10 m distributed on a slope and crossing the SRICCE (denoted by F_{cc} in Fig. 4c) at 456 m from the western end of the profile.

Figure 4 shows the measured data and the interpretative results. The interpretative model (Fig. 4c) has a RMS relative error of 5.8% indicating medium fit between the measured and the calculated data, and implying that the results are acceptable. Figure 4c shows that the strata are

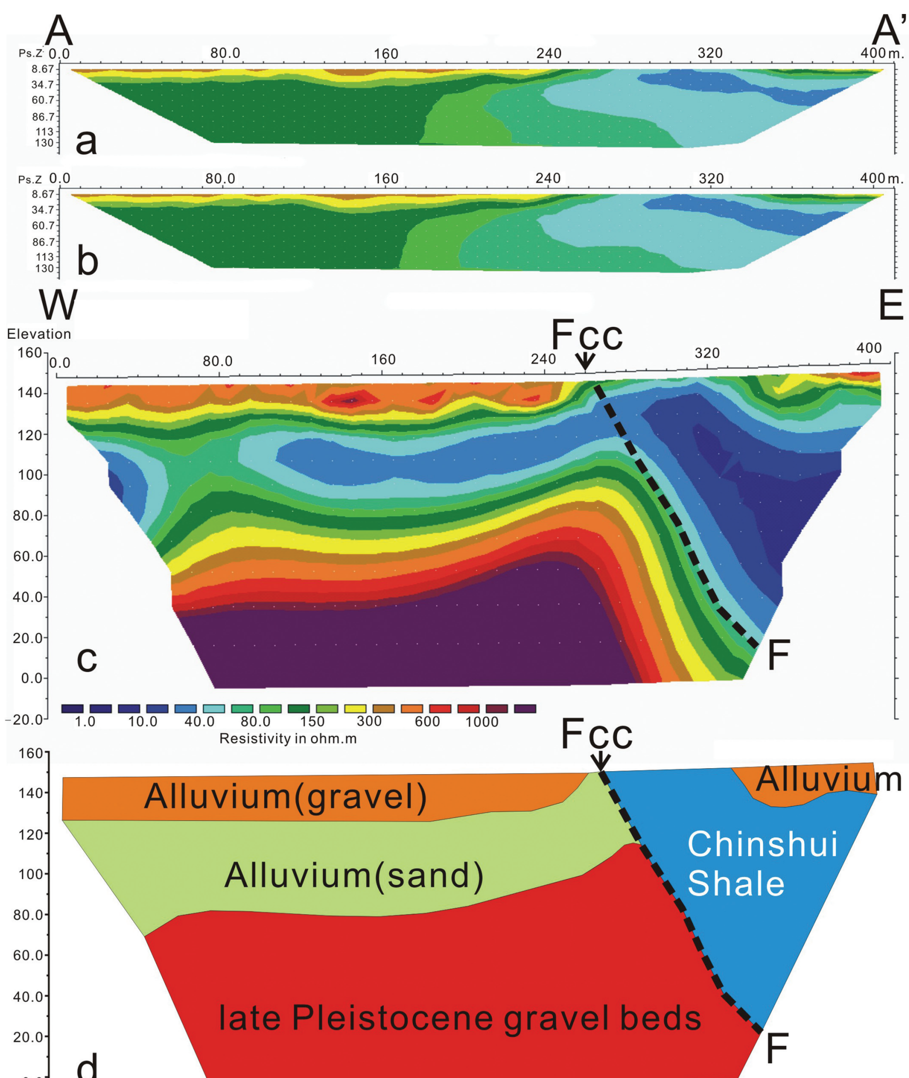

Fig. 3. Measured data and interpreted results of Profile A-A'. (a) Measured apparent resistivity pseudosection; (b) Calculated apparent resistivity pseudosection; (c) Interpretative model; and (d) Geological section deduced from (c). F_{cc}: surface rupture induced by the 1999 Chi-Chi earthquake. F: the main fault zone of the Chelungpu fault system in which the Chi-Chi earthquake rupture is involved, where the Chinshui Shale thrusted on the alluvium and the late Pleistocene gravel beds.

composed of a high resistivity layer (> 200 Ω-m, colored in red and yellow) at the top and a very-low resistivity layer (< 40 Ω-m, colored in dark blue) at the bottom generally, except for the part to the east of the SRICCE where a low resistivity layer presents at the top, instead of the high resistivity layer. The boundary between sections with and without the upper high resistivity layer is an east dipping zone beneath the SRICCE as denoted by F_2 in Fig. 4c. This boundary is suggested to be the subsurface fault zone associated with the Chi-Chi earthquake and is called the Chi-Chi earthquake rupture; it can be correlated to the Shihkang fault (Chen et al. 2003).

The upper high resistivity layer is confirmed to be the gravel beds of the lateritic terrace deposits, because laterite and gravels are widely exposed on the ground and throughout erosion trenches. The very-low resistivity layer at the bottom is once again suggested to be the Chinshui Shale, which has very-low resistivity (< 40 Ω-m) as measured on the outcrops of the Chinshui Shale on the stream bed. The stratum to the east of the SRICCE has a resistivity of 40 - 100 Ω-m, which is slightly higher than that of the Chinshui Shale. Hence, this is interpreted as the Cholan Formation based on the resistivity spectra of rocks and the formation sequence in the study area. The geological section of the profile deduced from the resistivity structures is shown in Fig. 4d. It shows the fault of the Chi-Chi earthquake rupture developing in the Cholan Formation with its top overlying the lateritic terrace deposits.

4.3 Profile C-C’

Profile C-C’ is situated to the west of Profile B-B’ in

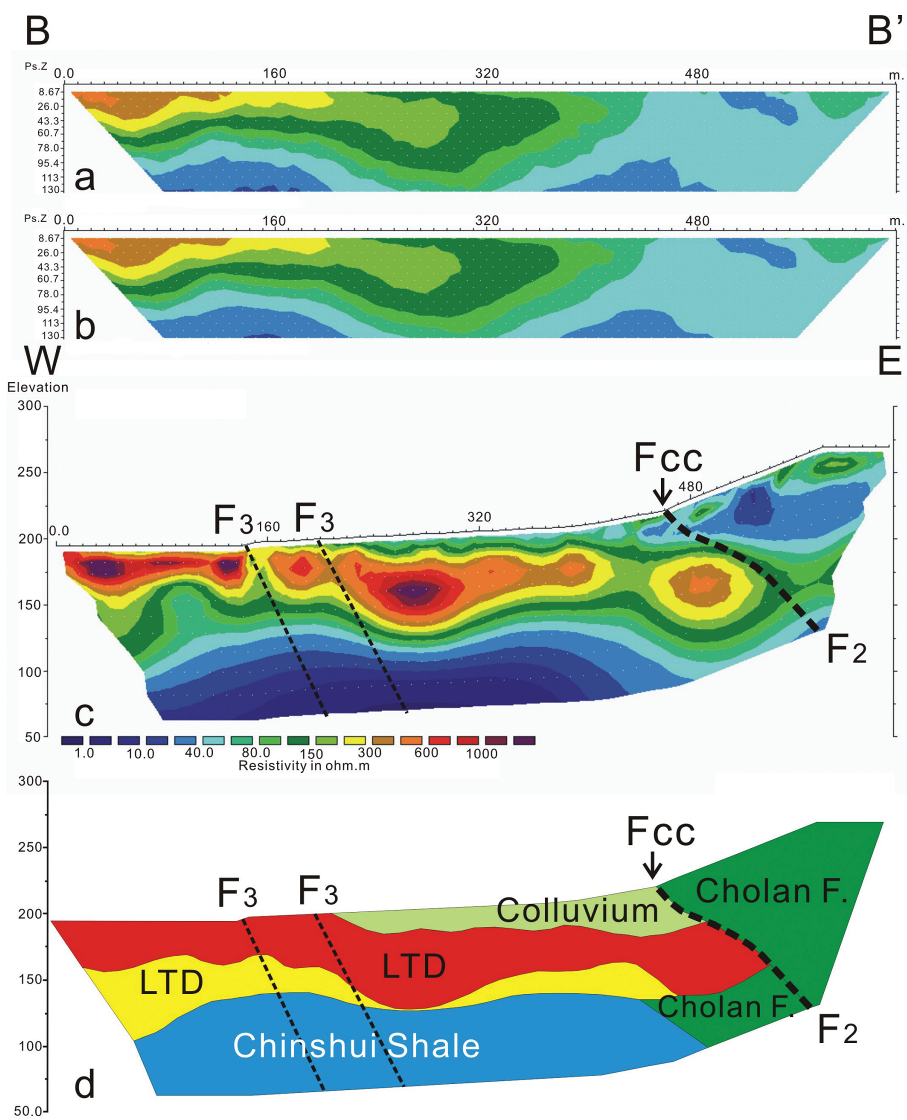

Fig. 4. Measured data and interpreted results of Profile B-B’. (a) Measured apparent resistivity pseudosection; (b) Calculated apparent resistivity pseudosection; (c) Interpretative model; and (d) Geological section deduced from (c). F_{cc}: surface rupture induced by the 1999 Chi-Chi earthquake; F_2: subsurface rupture associated with the Chi-Chi earthquake; LTD: the lateritic terrace deposits; and F_3: minor fault.

the central part of the study area (Fig. 1). It has a length of 315 m consisting of 64 sounding electrodes at equi-intervals of 5 m spread along a line in the same direction as Profile B-B'. It crosses the terrace scarp (denoted by F_t in Fig. 5c) at 80 m from the western end of the profile.

The observed data and the interpretative results of the profile are shown in Fig. 5. The interpretative results have a RMS relative error of 4.1% indicating good fit between the measured and the calculated apparent resistivities, and implying the interpretative results are acceptable. The interpretative model (Fig. 5c) indicates that the strata can be divided into western and eastern parts by resistivity structures. The western part is composed of a thick (> 100 m) high resistivity (300 - 1200 Ω-m) layer dominantly and a thin (< 15 m) medium resistivity layer on the top. The eastern part is composed of three layers, the top layer has a high resistivity of 600 ~ 1500 Ω-m with a thickness of 5 ~ 15 m, the middle layer has a resistivity of 5 ~ 40 Ω-m and the basal layer has a dominant resistivity of 50 ~ 150 Ω-m. The boundary between the middle and the basal layers dips eastwardly at an angle of about 20°.

Based on the outcrops of the strata, the medium resistivity layer on the top of the western part is correlated to the alluvial deposits, and the high resistivity layer on the top of the eastern part is correlated to the gravel beds of the lateritic terrace deposits. The very-low resistivity layer of

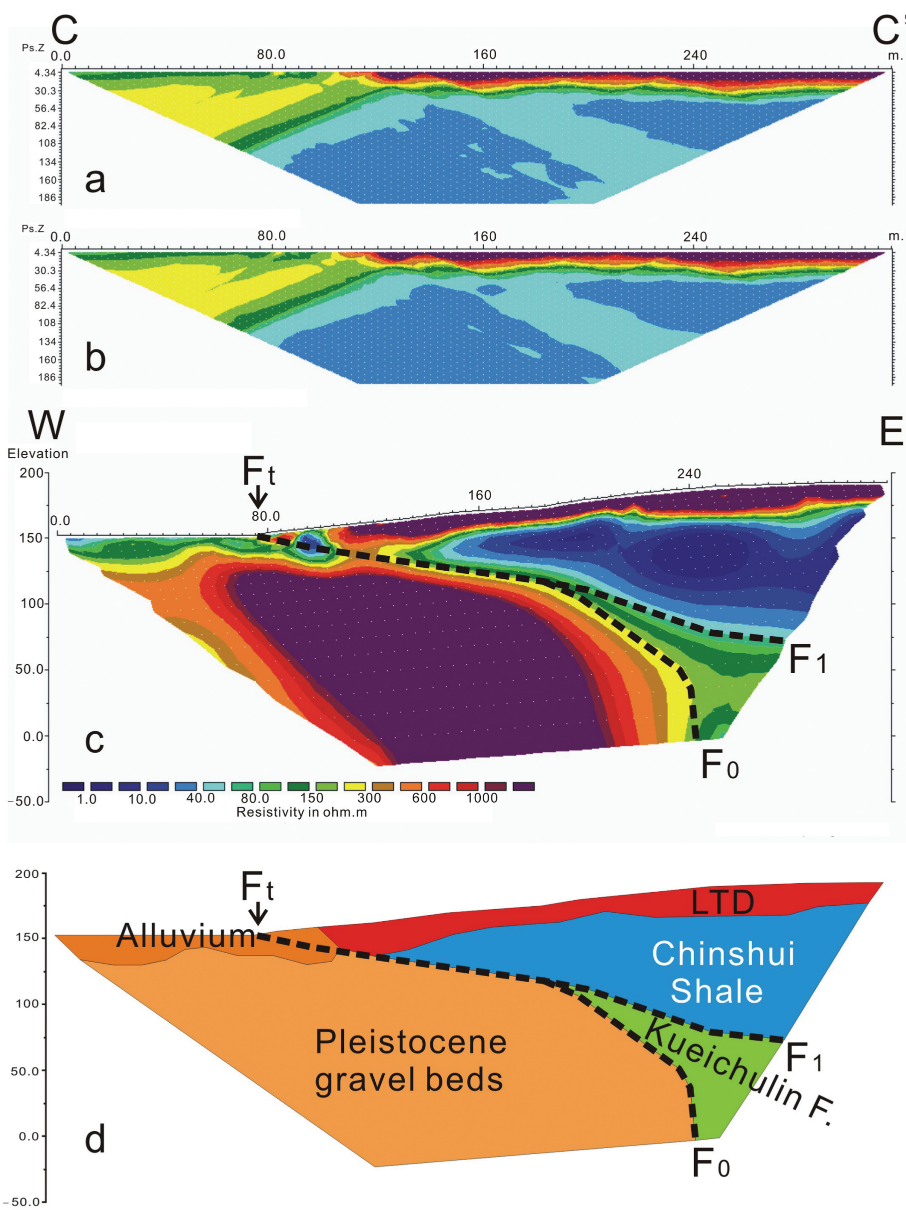

Fig. 5. Measured data and interpreted results of Profile C-C'. (a) Measured apparent resistivity pseudosection; (b) Calculated apparent resistivity pseudosection; (c) Interpretative model; and (d) Geological section deduced from (c). F_t: terrace scarp; F_1: Houli fault; and F_0: Sanyi fault.

the eastern part is suggested to be the Chinshui Shale for it has a very-low resistivity. The basal layer of the eastern part is suggested to be the Kueichulin Formation based on the rock formation sequence, resistivity spectra of rocks and a comparison between the resistivity profile and the seismic sections conducted in the study area (Wang et al. 2002; Chen et al. 2003). The geological section deduced from the resistivity structures is shown in Fig. 5d.

4.4 Profile D-D’

Profile D-D’ is situated on a slope in the northern part of the study area (Fig. 1). It consists of 51 sounding electrodes at equi-intervals of 10 m spread along a N93°E trendline 500 m long that crosses the SRICCE (denote by F_{cc} in Fig. 6c) 328 m from the western end of the profile.

Figure 6 shows the observed data and the interpreted results of the profile. The interpretative results have a RMS relative error of 4.4% indicating good fit between the measured and the calculated apparent resistivities, and implying the interpretative results are acceptable. The interpretative model (Fig. 6c) shows that a high resistivity (> 300 Ω-m) layer exists on the western to central top and terminates at the SRICCE. An east dipping boundary F_2 stretching from the SRICCE can be depicted as shown in Fig. 6c. It separates a low resistivity (25 ~ 60 Ω-m) block in the east from a medium resistivity (80 ~ 300 Ω-m) layer in the west. The boundary F_2 is interpreted as being the subsurface rupture associated with Chi-Chi earthquake. In the western to central part, the top high resistivity layer is underlain by a very-

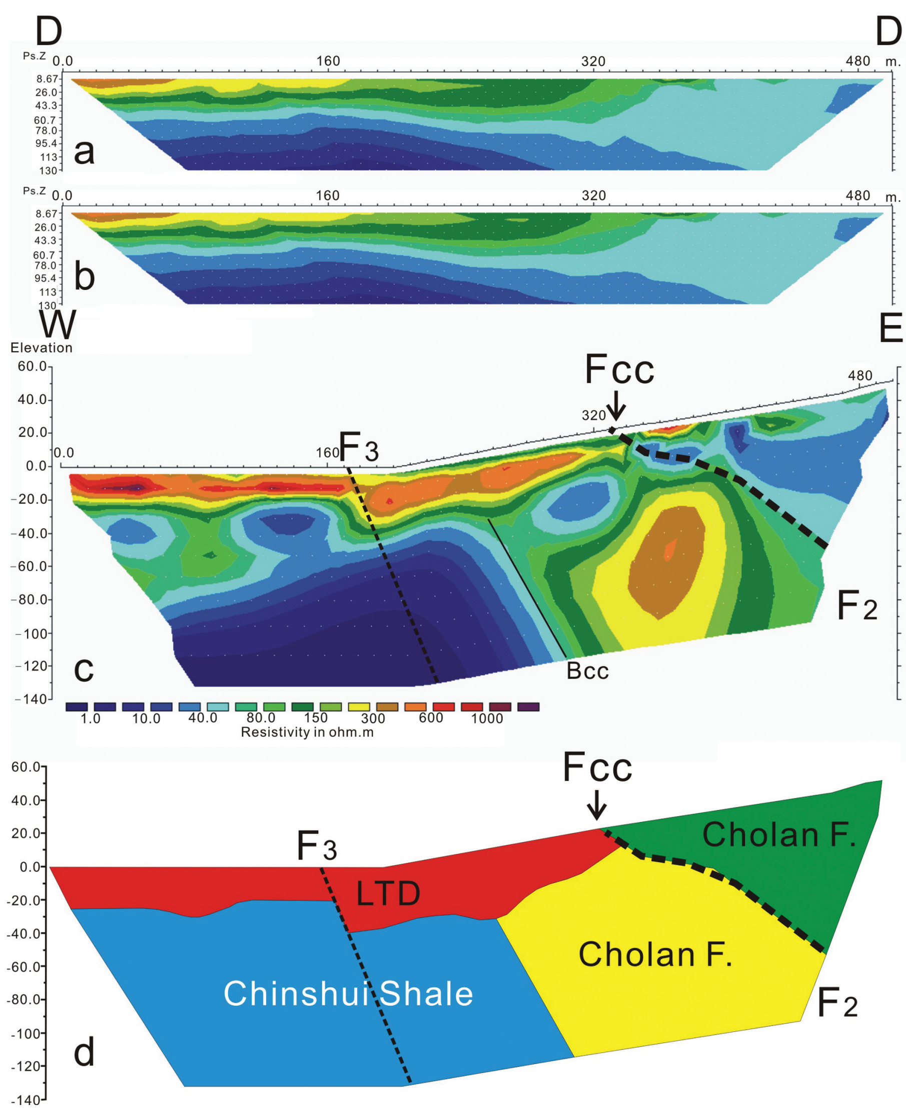

Fig. 6. Measured data and interpreted results of Profile D-D’. (a) Measured apparent resistivity pseudosection; (b) Calculated apparent resistivity pseudosection; (c) Interpretative model; and (d) Geological section deduced from (c). F_{cc}: surface rupture induced by the 1999 Chi-Chi earthquake; F_2: Chi-Chi earthquake rupture [it developed in the Cholan Formation, the uppermost part of the Cholan Formation overlies the lateritic terrace deposits (LTD)]; and F_3: minor fault.

low resistivity block (8 - 40 Ω-m, colored in dark blue) and the medium resistivity layer (colored in yellow) to the west of F_2.

The high resistivity layer on the top of the western to central part can be correlated to the gravel beds of lateritic terrace deposits that appear on the ground. Based on the resistivity spectra of rocks, the very-low resistivity block at the bottom of the western part is interpreted as being the Chinshui Shale for its very-low resistivity characteristics. The medium resistivity layer to the east of the Chinshui Shale is suggested to be a layer of sandstone of the Cholan Formation. The low resistivity block to the east of F_2 (colored in green) is suggested to be a block of sandstone and shale in alternation of the Cholan Formation. The geological section of the profile deduced from the resistivity structures is shown in Fig. 6d. It shows the fault of the Chi-Chi earthquake rupture developing in the Cholan Formation, and the uppermost region the Cholan Formation thrusting onto the lateritic terrace deposits.

4.5 Profile E-E'

The eastward trending Profile E-E' consists of 32 sounding electrodes spread at 10-m intervals along a line 310 m long on the terrace in the northern part of the study area (Fig. 1). The western end of the profile is located at the western topographic riser of the terrace.

The measured data and the interpretative results of the profile are shown in Fig. 7. The interpretative results have a RMS relative error of 6.6% indicating medium fit between the measured and the calculated apparent resistivities, and implying the interpretative results are acceptable. The interpretative model (Fig. 7c) shows that the ground can be divided into three layers of different resistivity. The top layer has a resistivity higher than 300 Ω-m, the middle layer has a dominant resistivity of 10 - 40 Ω-m and the basal layer

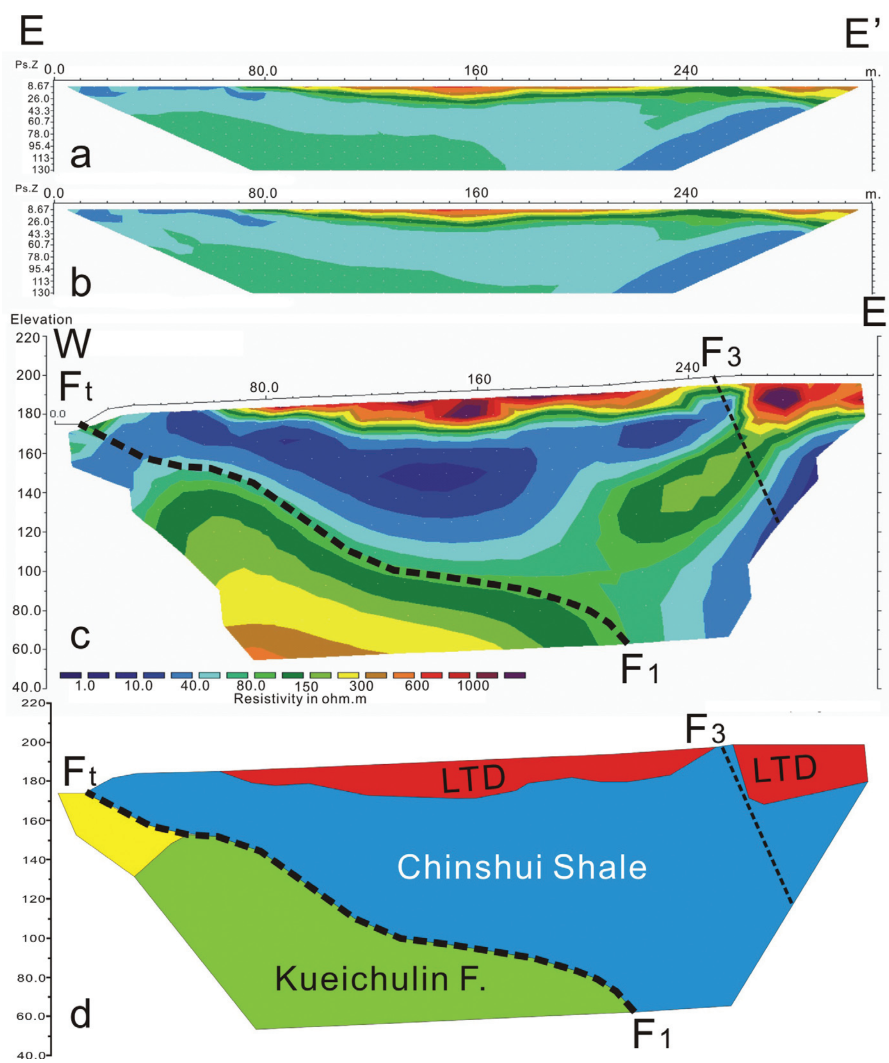

Fig. 7. Measured data and interpreted results of Profile E-E'. (a) Measured apparent resistivity pseudosection; (b) Calculated apparent resistivity pseudosection; (c) Interpretative model; and (d) Geological section deduced from (c). F_t: terrace scarp; F_1: the main shear zone of the Chelungpu fault system (Houli fault) where the uppermost part of the Chinshui Formation thrusted on the Alluvium; and F_3: minor fault.

has a dominant resistivity of 100 - 400 Ω-m. The boundary between the middle and the basal layers (labeled by F_1 in Fig. 7c) dips eastwardly and emerges at the terrace scarp (denoted by F_t in Fig. 7c).

The top layer of high resistivity can be correlated to the gravel beds of the lateritic terrace deposits that appear on the ground. The middle layer is interpreted as being the Chinshui Shale because of its very-low resistivity characteristics. These resistivities are consistent with the apparent lithology of gravel on the top and shale at the bottom on the walls of an evacuation about 30 m to the south of the profile. The basal layer is suggested to be the Kueichulin Formation based on the resistivity spectra of rocks, the rock formation sequence and comparisons with seismic sections conducted in the study area (Wang et al. 2002; Chen et al. 2003).The boundary between the Chinshui Shale and the Kueichulin Formation is suggested to be the Chelungpu fault. The geological section of the profile deduced from the resistivity structures is shown in Fig. 7d.

4.6 Profile F-F'

The eastward trending Profile F-F' is situated to the west of Profile E-E' in the northern part of the study area (Fig. 1). It consists of 24 sounding electrodes at 10-m equi-intervals spread on the alluvial plain.

The observed apparent resistivity pseudosection and the interpreted results are shown in Fig. 8. The interpreta-

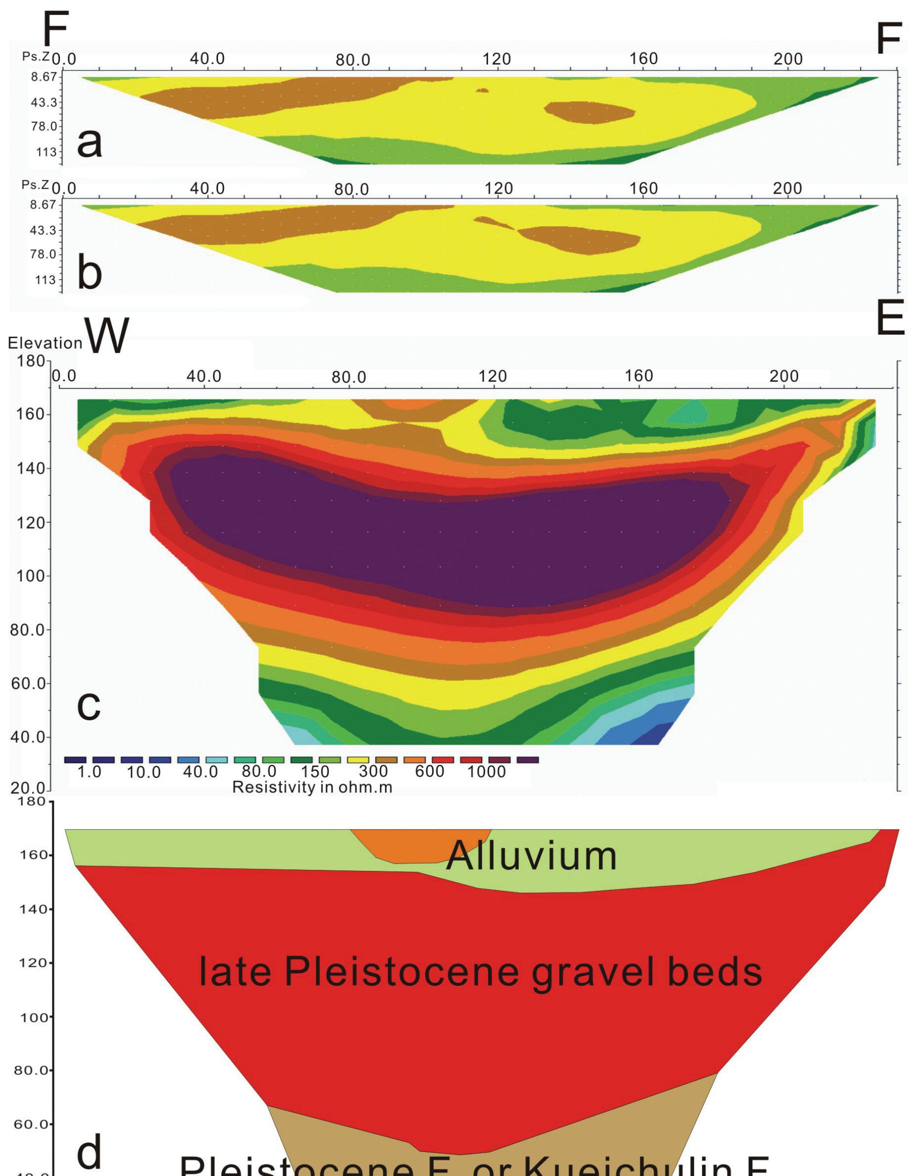

Fig. 8. Measured data and interpreted results of Profile F-F'. (a) Measured apparent resistivity pseudosection; (b) Calculated apparent resistivity pseudosection; (c) Interpretative model; and (d) Geological section deduced from (c).

tive results have a RMS relative error of 3.5% indicating good fit between the measured and the calculated apparent resistivities, and implying the results are acceptable. The interpretative model (Fig. 8c) shows the ground having a high resistivity (500 - 1200 Ω-m) layer dominantly. The high resistivity layer is overlain by a less-resistive (80 - 300 Ω-m) layer and underlain by a layer of resistivity from 300 to 40 Ω-m decreases with depth.

The less-resistive upper layer has a thickness of 10 - 20 m and is correlated to the alluvial deposits that appear on the ground. Based on the resistivity spectra of rocks and the formation sequence in the study area, the high resistivity layer is suggested to be late Pleistocene gravel beds. As for the layer of resistivity 300 ~ 40 Ω-m on the bottom, we cannot confirm what this geological formation is. It may be the Pleistocene formation or it may be the Kueichulin Formation. The geological section of the profile deduced from the resistivity structures is shown in Fig. 8d.

4.7 MT Soundings

Three magnetotelluric sounding results (labeled MT5, 6, and 25) are selected from megnetotelluric prospecting (Cheng et al. 2006) to assist with the correlating of the resistivity structures to the rock formations, especially at depth.

The MT25 site is located about 250 m west of the Fengyuan well and is about 150 m east of the SRICCE (Fig. 9). The sounding results of MT25 and the rock formations with fracture zones recognized from the cores of the Fengyuan well are shown in Fig. 9. The interpretative models of the TE mode and the TM mode are similar in resistivity structure. They have low resistivity layers in the upper part and high resistivity layers in the lower part. A slight difference between them implies that the strata are anisotropic or in a dipping state. The interpretative model of the TE mode correlates better to the rock formations (Fig. 9c). The top very-low resistivity layer (5 ~ 50 Ω-m) above a depth of 90 m is correlated to the Chinshui Shale. The rupture induced by the Chi-Chi earthquake is depicted from the outcrop of the fault to the fracture zone found in the cores. The rupture is an east dipping zone; it cuts through the bottom of the very-low resistivity layer, implying that faulting occurred along the bottom of the Chinshui Shale. This result is the same as that found in the cores of the Fengyuan well. The Kueichulin Formation is correlated to layers below a depth of 90 m which have a resistivity of 50 ~ 400 Ω-m. Figure 9c shows that the main fracture zone in the Kueichulin Formation between drilling depths of 280 and 330 m (vertical depth 214 ~ 252 m) is well correlated to the low resistivity (50 ~ 100 Ω-m) layer at a depth of 160 ~ 210 m beneath the site of MT 25 along an eastward dipping zone. The resistivity range of 50 ~ 100 Ω-m for the fracture zone in the Kueichulin Formation is similar to that beneath the TCDP site (Cheng et al. 2006).

The MT5 site is located on the alluvial Plain (Fig. 1). The sounding results of the TE mode and the TM mode are shown in Fig. 10. These results show that the interpretative models of the TE and the TM modes are similar in resistivity structure, both of them have a high resistivity (> 400 Ω-m) layer below a depth of 70 m. They show that no layer of resistivity 50 ~ 400 Ω-m, the resistivity range corresponding to the Kueichulin Formation, exists below a depth of 70 m.

The MT6 site is located on the terrace (Fig. 1). The sounding results of the TE mode and the TM mode have a similar resistivity structural pattern (Fig. 11). They show that the strata below a depth of 400 m have a resistivity higher than 400 Ω-m. The strata between the depths of 160 and 400 m have a resistivity of 100 ~ 400 Ω-m, and the strata on the upper part (20 ~ 160 m) have a resistivity 5 ~ 100 Ω-m. The interpretative model of the TE mode is consistently better than that of the TM mode with the RIP results. The interpretative model of the TE mode has a very-low resistivity (5 ~ 50 Ω-m) upper layer; i.e., the top 20 ~ 110 m. This segment is suggested to be the Chinshui Shale for its very-low resistivity. Based on resistivity spectra and the formation sequence, the segment at a depth of 110 ~ 400 m with resistivity 50 ~ 400 Ω-m is suggested to be the Kueichulin Formation and the segment below a depth of 400 m with resistivity higher than 400 Ω-m is suggested to the Pleistocene Formation.

5. DISCUSSIONS

5.1 Geological Structures beneath the Terrace

The interpretative geological sections of profiles A-A' and C-C' (Figs. 3d and 5d) show that the younger Quaternary deposits in the west are overlain by the older Chinshui Shale in the east with an eastward dipping boundary indicating the boundary is a thrust fault. Figure 3 shows that the fault dips eastwardly at an angle of about 60°. Figures 5 and 7 show that the fault developed along the boundary between the Chinshui Shale on the hanging wall and the Kueichulin Formation on the footwall in depth. It dips eastwardly at an angle of 20° ~ 30° as denoted by F_1 in Figs. 5d and 7d. This fault was also found in a seismic section conducted along the Tali Stream (Wang et al. 2002).

The Kueichulin Formation has been dragged (Fig. 7) and terminated (Fig. 5) beneath the terrace implying that a fault exists on its bottom. Figure 5d shows that the Kueichulin Formation overlies the Pleistocene formation with an eastward dipping boundary indicative of a thrust (denoted by F_0 in Fig. 5d). Referring to the TCDP core (Cheng et al 2006), this fault is correlated to the Sanyi fault. Figure 5d shows that the Sanyi fault and the Houli fault merged together into a fault zone at a shallow depth beneath the terrace. This fault zone is named the main shear zone of the Chelungpu fault system.

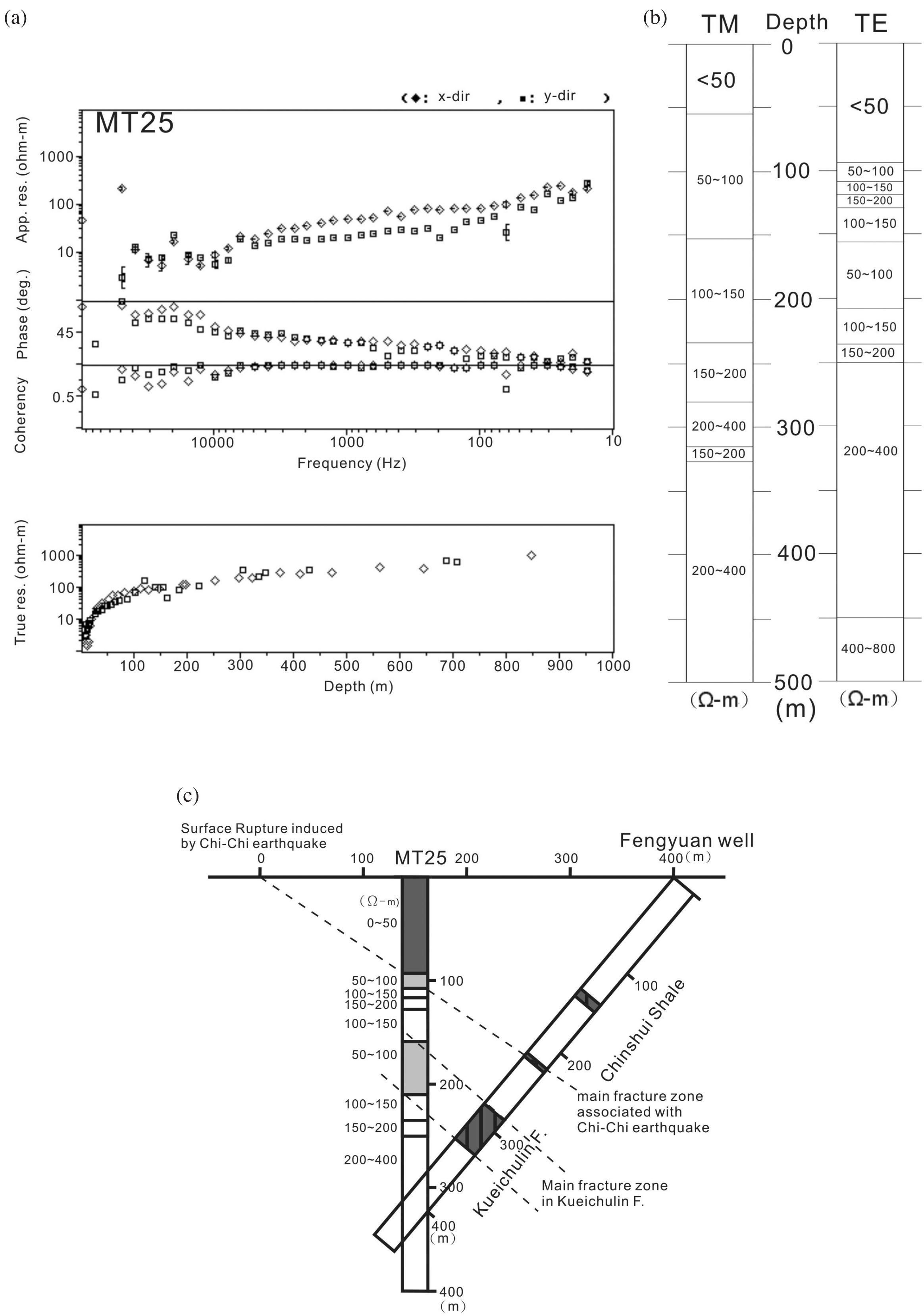

Fig. 9. (a) The MT sounding results of MT25; (b) Resistivity columns of MT25 interpreted from the data of TE and TM modes; and (c) The resistivity column of TE mode and the rock formations recognized from the cores of the Fengyuan well.

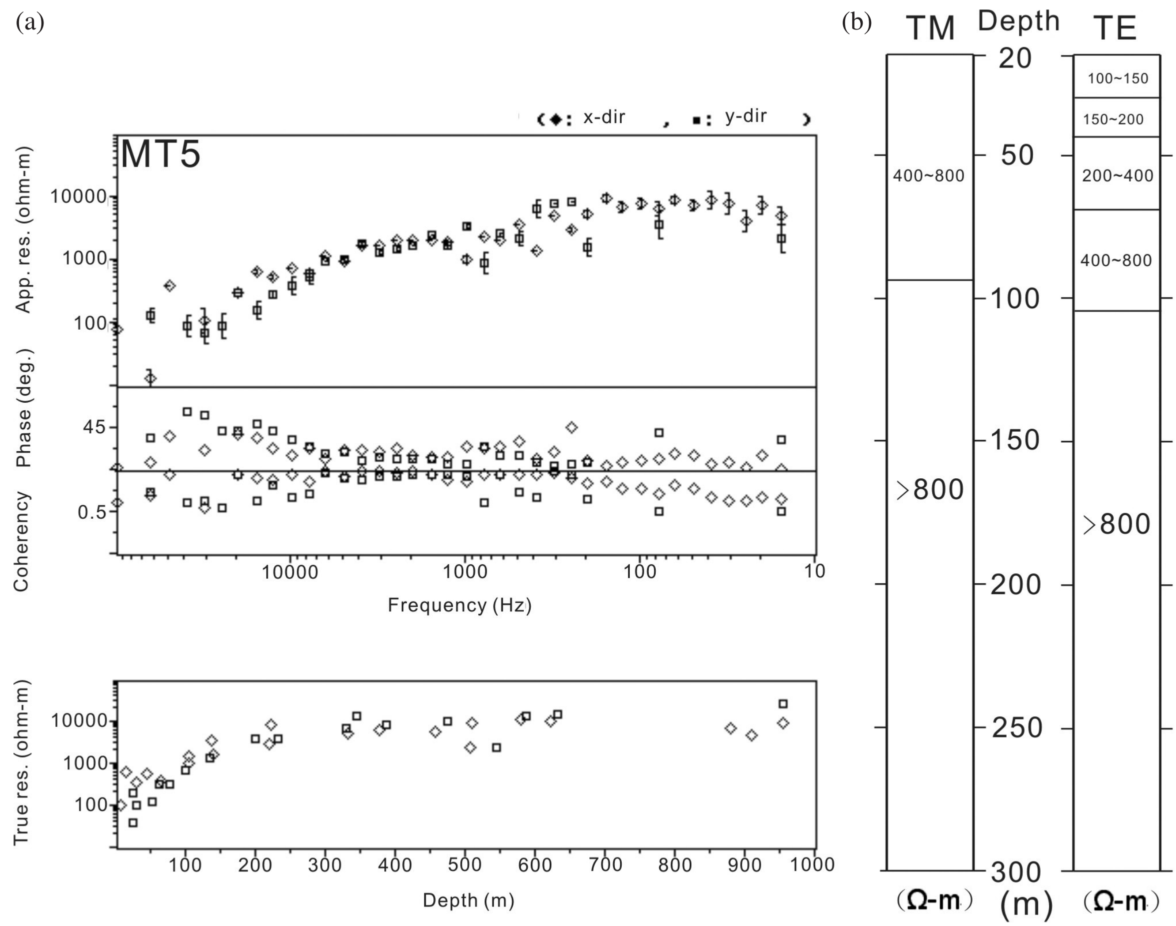

Fig. 10. (a) The MT sounding results of MT5; and (b) Resistivity columns of MT5 interpreted from the data of TE and TM modes.

5.2 Rupture Associated with the Chi-Chi Earthquake and the Shihkang Fault

The subsurface rupture induced by the Chi-Chi earthquake was found in Profiles A-A', B-B', and D-D'. In Profile A-A', it exhibits typical contact for the Chelungpu fault, that is, the Chinshui Shale overlies the Quaternary formation with an east dipping boundary. This indicates that the Chi-Chi earthquake rupture coincided with the main shear zone of the Chelungpu fault system. In Profiles B-B' and D-D', the Chi-Chi earthquake rupture developed in the Cholan Formation on the hanging wall of the main shear zone. In this segment, the Chi-Chi earthquake rupture is correlated to the Shihkang fault (Chen et al. 2001).

In Profiles B-B' and D-D', the gravel layer of the lateritic terrace deposits borders the Chi-Chi earthquake rupture in the east. The forming of the gravel layer looks to be related to the relative uplift of the eastern block of the fault. The terrace gravel layer is about 70 m thick in Profile B-B', which is to the south while for the more northward Profile D-D' it is 30 m thick. This implies that the relative uplift is about 70 m in the south and about 30 m in the north of the study area. This difference in relative uplift might be caused by differential uplifting of the fault at different segments, or by different sharing of the uplift into several blocks.

If an earthquake event resulted in a faulting throw of 2 m, an approximation of the magnitude of faulting induced by the Chi-Chi earthquake (Chang et al. 1999), then more than fifteen faulting events of this magnitude had occurred along the Chi-Chi earthquake rupture prior to the 1999 Chi-Chi earthquake. In other words, the Shihkang fault is an active fault where faulting has occurred many times since the lateritic terrace gravel layer was formed in the late Pleistocene.

The Chi-Chi earthquake rupture coincides with the main shear zone of the Chelungpu fault system in the south of the study area, indicating the Shihkang fault is a branch of the Chelungpu fault system.

5.3 Inconsistency between the Interpretative Results of MT5 and Profile F-F'

The sites of MT5 and Profile F-F' are both located on the alluvial plain and close to one another (Fig. 1), but the interpretative results are inconsistent between 100 and 130 m down. The interpretative model of Profile F-F' shows that

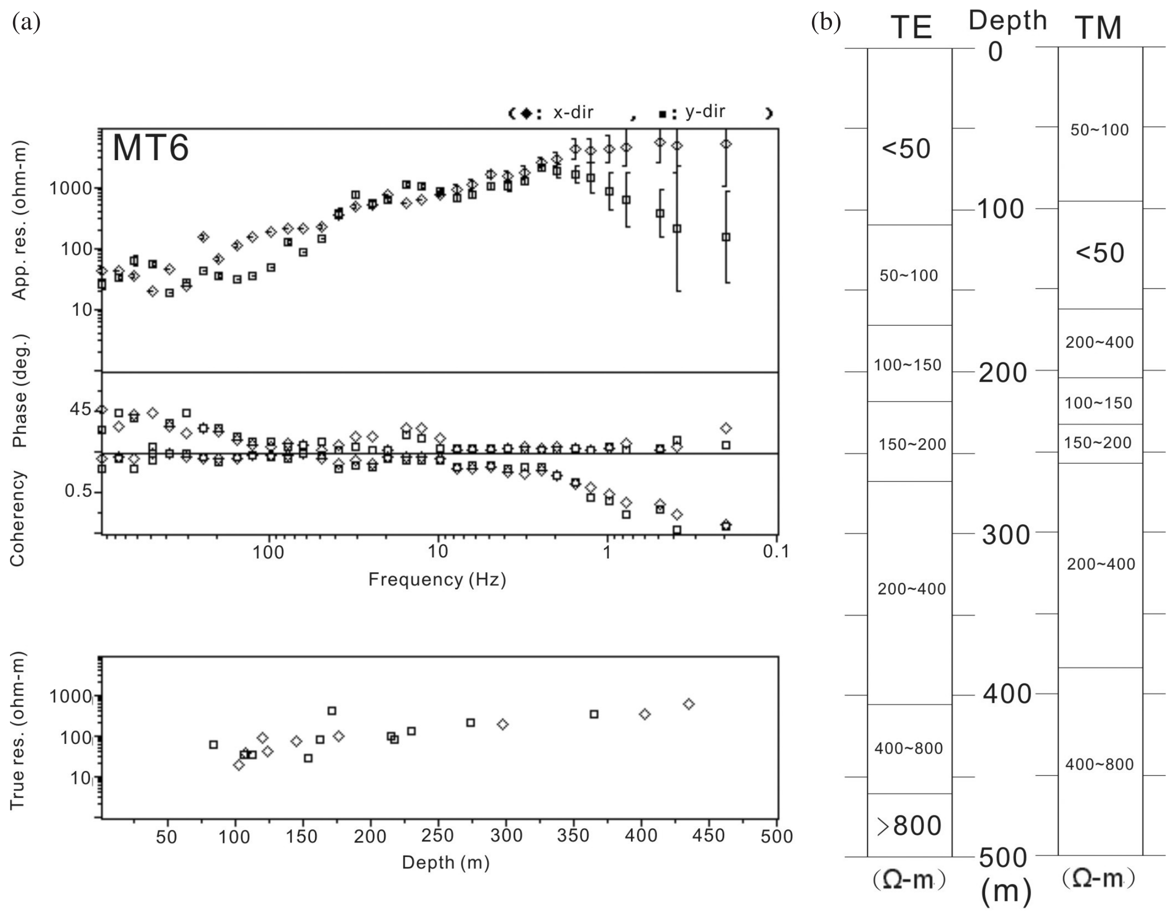

Fig. 11. (a) The MT sounding results of MT6; and (b) The resistivity columns of MT6 interpreted from the data of TE and TM modes.

the strata contain a layer of resistivity 50 ~ 400 Ω-m below a depth of 100 m (Fig. 8). In contrast, the interpretative model of MT5 shows that the strata below a depth of 70 m have a resistivity higher than 400 Ω-m. This inconsistency may be caused by local effect due to lateral heterogeneity and anisotropy of the strata. It may also be caused by the different response of the signals they received. The RIP data are derived from electric field signals generated from artificial alternative DC current. The magnetotelluric data are derived from the signals of electromagnetic fields of frequency band 10^5 ~ 1 Hz generated in nature.

The RIP method has a high data density so that a thin layer can be resolved. But a thin layer may be neglected in the interpretation of magnetotelluric data, especially in the case of noisy data measured in the high-frequency band, which are the correspondences of the shallow strata.

5.4 Extent of the Kueichulin Formation

The Kueichulin Formation is overlain by the Chinshui Shale beneath the terrace (Figs. 5d and 7d). It dips eastwardly to a depth ranging from 1313 to 1707 m beneath the TCDP site, where the Kueichulin Formation is overlain by the Chinshui Shale with the major fracture zone associated with Chi-Chi earthquake as the boundary, and is underlain by the Cholan Formation with the Sanyi fault as the boundary.

In the middle and the southern parts of the study area, the Kueichulin Formation seems to be absent at shallow depth beneath the alluvial plain because no layer of resistivity corresponding to the Kueichulin Formation (50 ~ 400 Ω-m) is found in Profiles A-A’ and C-C’. These results are inconsistent with the interpretative results of seismic sections in which the Kueichulin Formation extends beyond the terrace scarp and exists beneath the alluvial plain (Wang et al 2002; Chen et al 2003). But in the northern part of the study area, a layer of resistivity 50 ~ 400 Ω-m below a depth of 100 m is found in Profile F-F’. This layer of resistivity 50 ~ 400 Ω-m should not be a thick layer considering the interpretative results of MT5. We cannot confirm what the geological formation it is. It may be a layer of the late Pleistocene formation or a layer of the Kueichulin Formation.

6. CONCLUSION

Combining resistivity measurements on outcrops of strata and the correlation between resistivity structures and rock formations recognized from drilling cores as well as outcrops of strata, resistivity spectra of rock formations in the Taichung area are used to investigate the subsurface structures of the Chelungpu fault. The alluvial gravel layer and the alluvial sand layer have a dominant resistivity of 200 ~ 600 and 30 ~ 150 Ω-m, respectively. The gravel beds of the lateritic terrace deposits have a dominant resistivity of 300 ~ 1200 Ω-m. The layer underlying the alluvium in the plains area, which is suggested to be the late Pleistocene gravel beds has a dominant resistivity of 150 ~ 1200 Ω-m. The Cholan Formation and the Chinshui Shale have a dominant resistivity of 40 ~ 100 and 8 ~ 40 Ω-m, respectively. The Kueichulin Formation has a dominant resistivity 50 ~ 150 Ω-m and may reach to 400 Ω-m in some areas or for some special lithology.

The interpretative results of the RIP data show that the Chelungpu fault is a complex fault system consisting of two major thrust faults, several minor faults accompanied with fractures in the Taichung area. The two major thrust faults are the main shear zone of the Chelungpu fault system lying in the west and the Chi-Chi earthquake rupture lying in the east. They are 300 - 800 m apart on the ground surface and trend in a N-S direction. In the south of the study area, the main shear zone and the Chi-Chi earthquake rupture are coincident in location.

The main shear zone is composed of the Houli fault and the Sanyi fault which merged together beneath the terrace and outcropped along the terrace scarp. It dips eastwardly at an angle of 20° - 60° and has a cumulate throw of several thousands of meters.

The Chi-Chi earthquake rupture can be correlated to the Shihkang fault. It is a branch of the Chelungpu fault system which developed in the Cholan Formation on the hanging wall of the main shear zone in the Taichung area. It dips eastwardly at an angle of 40° - 60°. It has a cumulate throw of several tens of meters implying that the fault was formed earlier than the 1999 Chi-Chi earthquake and it is evident that thrusting events have occurred there many times. It has been very active recently and may become the dominant active fault zone in the northern segment of Chelungpu fault system.

Acknowledgements The authors are grateful to the diligent field crew of the Geoelectric Group at the Institute of Geophysics, National Central University. This study is supported by the National Science Council of Taiwan under grants: NSC90-2119-M-008-008, NSC91-2119-M-008-016, and NSC94-2119-M-008-004.

REFERENCES

Chang, H. C., C. W. Lin, and S. T. Lu, 1999: The report of a field survey of the 921 earthquake. Central Geological Survey, MOEA, Taiwan. (in Chinese)

Chang, S. L., 1971: Subsurface geologic study of the Taichung basin. *Petrol. Geol. Taiwan*, **8**, 21-45.

Chen, W. S., B. S. Huang, Y. G. Chen, Y. H. Lee, C. N. Yang, C. H. Lo, H. C. Chang, Q. C. Sung, N. W. Huang, C. C. Lin, S. H. Sung, and K. J. Lee, 2001: 1999 Chi-Chi earthquake: A case study on the role of thrust-ramp structures for generating earthquakes. *Bull. Seismol. Soc. Am.*, **91**, 986-994.

Chen, W. S., Y. G. Chen, R. C. Shih, T. K. Liu, N. W. Huang, C. C. Lin, S. H. Sung, and K. J. Lee, 2003: Thrust-related river terrace development in relation to the 1999 Chi-Chi earthquake rupture, western foothills, central Taiwan. *J. Asian Earth Sci.*, **21**, 473-480.

Cheng, P. H., 1990: Electrostratigraphic study of the Quaternary Formations in the Houli tableland. *Proc. Geol. Soc. China*, **33**, 127-142.

Cheng, P. H., C. H. Yang, J. I. You, and J. S. Shieh, 2002: An electric resistivity study of the Chelungpu fault in the Tsaotun area, central Taiwan. *Terr. Atmos. Ocean. Sci.*, **13**, 375-386.

Cheng, P. H., A. T. S. Lin, Y. I. Ger, and K. H. Chen, 2006: Resistivity structure of the Chelungpu fault in the Taichung area, Taiwan. *Terr. Atmos. Ocean. Sci.*, **7**, 547-561.

deGroot-Hedlin, C. and S. Constable, 1990: Occam's inversion to generate smooth, two-dimensional models from magnetotelluric data. *Geophysics*, **55**, 1613-1624.

Ho, C. S., 1975: An introduction to the geology of Taiwan explanatory text of the geologic map of Taiwan. MOEA, Taiwan, 153 pp.

Ho, H. C. and M. M. Chen, 2000: Explanatory text of the geologic map of Taiwan, sheet Taichung. Central Geological Survey, MOEA, Taiwan, 65 pp.

Huang, S. T., J. C. Wu, J. H. Hung, and H. Tanaka, 2002: Studies of sedimentary facies, stratigraphy, and deformation structures of the Chelungpu fault zone on cores from drilled wells in Fengyuan and Nantou, central Taiwan. *Terr. Atmos. Ocean. Sci.*, **13**, 253-278.

Huang, W. J., Z. Y. Chen, S. Y. Liu, Y. H. Lin, C. W. Lin, and H. C. Chang, 2000: Surface deformation models of the 1999 Chi-Chi earthquake between Tachiachi and Toupienkengchi, central Taiwan. Special issue for the Chi-Chi earthquake, 1999, Central Geological Survey, MOEA, Taiwan, 63-87.

Keller, G. V. and F. C. Frischknecht, 1966: Electrical methods in geophysical prospecting. Pergamon Press Inc., 517 pp.

Lee, J. F., C. S. Hou, C. C. Lin, and T. C. Lai, 1999: The Chelungpu fault and the 921 Chi-Chi large earthquake. Special issue of the Chi-Chi large earthquake, Central Weather Bureau and the Geophysical Soc. of China, Taiwan, 7-36. (in Chinese)

Lin, C. W., H. C. Chang, S. T. Lu, T. S. Shin, and W. J. Huang, 2000: An introduction to the active faults of

Taiwan. 2nd Ed., Central Geological Survey, MOEA, Taiwan, 129 pp. (in Chinese)

Loke, M. H. and R. D. Barker, 1996: Rapid least-squares inversion of apparent resistivity pseudosection by a quasi-Newton method. *Geophys. Prospect.*, **44**, 131-152.

Meng, C. Y., 1963: San-I overthrust. *Petrol. Geol. Taiwan*, **2**, 1-20.

Nabighian, M. N., 1988: Electromagnetic methods in applied geophysics-Theory. Vol. 1, Soc. Exploration Geophysicsts, 513 pp.

Tanaka, H., C. Y. Wang, W. M. Chen, A. Sakaguchi, K. Ujiie, H. Ito, and M. Ando, 2002: Initial science report of shallow drilling penetrating into the Chelungpu fault zone, Taiwan. *Terr. Atmos. Ocean. Sci.*, **13**, 227-251.

Tong, L. T. and C. H. Yang, 1990: Incorporation of topography into two-dimensional resistivity inversion. *Geophysics*, **55**, 354-361.

Wang, C. Y., C. L. Li, F. C. Su, M. T. Leu, M. S. Wu, S. H. Lai, and C. C. Chern, 2002: Structural mapping of the 1999 Chi-Chi earthquake fault, Taiwan by seismic reflection methods. *Terr. Atmos. Ocean. Sci.*, **13**, 211-226.